A Comparison of Four New Time-Domain Techniques for Discriminating Monomorphic Ventricular Tachycardia from Sinus Rhythm Using Ventricular Waveform Morphology

Robert D. Throne, Janice M. Jenkins, *Senior Member, IEEE*, and Lorenzo A. DiCarlo

***Abstract*—Electrical management of intractable tachycardia via implantable antitachycardia devices has become a major form of therapy. Newly advanced methods of ventricular tachycardia detection propose examination of changes in intraventricular electrogram morphology in addition to or in combination with earlier rate-based detection algorithms. Unfortunately, most of the proposed morphology analysis techniques have computational demands beyond the capabilities of present devices or may be adversely affected by amplitude and baseline fluctuations of the intraventricular electrogram.**

We have designed four new computationally efficient time-domain algorithms for distinguishing ventricular electrograms during monomorphic ventricular tachycardia (VT) from those during sinus rhythm using direct analysis of the ventricular electrogram morphology. All four techniques are independent of amplitude fluctuations and three of the four are independent of baseline changes. These new techniques were compared to correlation waveform analysis, a previously proposed method for distinction of VT from sinus rhythm. Evaluation of these four new algorithms was performed on data from 19 consecutive patients with 31 distinct monomorphic ventricular tachycardia morphologies. Three of the algorithms performed as well or better than correlation waveform analysis but with one-tenth to one-half the computational demands.

Introduction

THERE are many proposed methods for differentiating sinus rhythm from ventricular tachycardia (VT). Most early methods were based primarily on timing information which could be implemented in the existing hardware available in antitachycardia devices. Besides sustained high rate, simple measures derived from rate have been examined for more precise detection of ventricular tachycardia. These include the maximal rate of sinus tachycardia compared to the onset of VT [1], changes in cycle length at the onset of VT [2], and rate stability during VT [3]. Among the methods most widely used for detection of VT in single chamber antitachycardia devices are rate, rate stability, and sudden onset [4]–[10].

Along with rate, morphology differences between ventricular electrograms during sinus rhythm and ventricular tachycardia are being investigated for more accurate discrimination. One commercially available device for treatment of VT uses rate alone or both rate and a probability density function (PDF) [11], [12] as an attempt to discriminate sinus rhythm from ventricular fibrillation. However, PDF has been less reliable in VT detection than it has been in detecting ventricular fibrillation.

Recently, investigators have proposed a variety of schemes for detection of VT based on analysis of the ventricular electrogram. Amplitude distribution analysis, a software algorithm similar to PDF, has been tested with limited success [10], [13]. Some success has been reported using the gradient pattern detection (GPD) method [14]–[16] which proposes discrimination of ventricular electrograms during sinus rhythm from those during VT using the order in which the first derivative of the ventricular depolarization crosses predetermined thresholds. Another technique proposed for detecting VT combines bandpass filtering, rectifying, amplitude scaling, and signal integration over a 5 s moving time window [17]. A feature extraction algorithm [18] utilizing the product of the peak amplitude difference (maximum − minimum) and duration (time between maximum and minimum) has been developed, but has been tested on only four patients. In other studies, the use of amplitude dV/dt and the −3 dB point of the frequency domain power spectrum have not been consistently successful in discriminating sinus rhythm from VT [19], [20]. Another method, the area of difference [19]–[22] has had successful results in 10 patients. However, the results may be adversely affected by fluctuations in electrogram amplitude and baseline changes [22].

Recently, correlation waveform analysis (CWA) has been proposed for differentiating sinus rhythm from VT [13]. CWA is independent of amplitude and baseline fluctuations, and produces an index of merit reflecting mor-

Manuscript received January 1, 1990; revised July 30, 1990. This work was supported in part by NSF under Grants EET-8351215, BCS-89090421, a grant from Medtronic, Inc., and NIH Grant HL35554.

R. D. Throne is with the Pritzker Institute of Medical Engineering, Chicago, IL 60616.

J. M. Jenkins is with the Medical Computing Laboratory, Department of Electrical Engineering, and Computer Science, University of Michigan, Ann Arbor, MI 48109.

L. A. DiCarlo is with the Cardiac Electrophysiology Laboratory, St. Joseph Mercy Hospital of the Catherine McAuley Health Center, Ann Arbor, MI 48106.

IEEE Log Number 9144681.

phological changes only. The computational demands of CWA are considerable, however, and implementation of this technique in an implantable device is problematic. Thus, we sought to develop alternate methods which might produce results similar to those of CWA but which are computationally simpler.

We present four new time-domain template matching methods for discriminating sinus rhythm from monomorphic ventricular tachycardia based solely on ventricular electrogram morphology. Three methods, the bin area method (BAM), the derivative area method (DAM), and the accumulated difference of slopes (ADIOS) are independent of fluctuations of the baseline in ventricular electrograms as well as changes in electrogram amplitudes. A fourth method, the normalized area of difference (NAD), is independent of amplitude changes but not baseline fluctuations. Like CWA, two methods (BAM, NAD) use the electrogram directly while the other two methods (DAM, ADIOS) utilize the first derivative of the ventricular waveform. The computational requirements of these methods range from one-tenth to one-half those of CWA.

Methods

Patient Population and Data Acquisition

Bipolar ventricular endocardial electrograms were recorded from 19 consecutive patients during elective clinical cardiac electrophysiology studies. From the start of our study each patient undergoing an electrophysiology study who had monomorphic VT induced was included, whether the underlying rhythm was sinus rhythm (16 patients) or atrial fibrillation (3 patients), and whether the patient was on an antiarrhythmic drug (15 patients) or not (4 patients). All distinct VT morphologies induced were examined; however, the same VT morphology reinduced during serial drug testing was not used, as this would be more a measure of the effects of drugs on the electrogram than of the detection methods. Patient information is given in Table I. Patients were studied in a fasting postabsorptive state after sedation with 1–3 mg of intravenous medazolam. After administering 1% lidocaine for local anesthesia, three 7 French side-arm sheaths (Cordis Corporation) were positioned in the right femoral vein using the Seldinger technique. Three 6 French quadrapoler electrode catheters with an interelectrode distance of 1 cm (USCI division, C. R. Bard, Inc.) were introduced and advanced under fluoroscopic guidance to the high right atrium (or right atrial appendage) and right ventricular apex. Two catheters were positioned in the right ventricular apex with one dedicated to pacing and the other to obtaining recordings from the distal electrode pair. All recordings were made with the patients lying supine. Immediately before programmed stimulation, a 12-lead electrocardiogram was recorded during sinus rhythm. Ventricular electrograms were recorded on FM magnetic tape (Hewlett-Packard Models 3968 and 3964A) from distal bipolar endocardial electrodes positioned in the right ventricular apex using amplifiers with filter settings of 0.5–500 Hz (Siemens Mingograf-7) or 1 to 500 Hz (Honeywell Electronics for Medicine). Tape speed was $3\frac{3}{4}$ in per second with a bandwidth of 0–1250 Hz. The recorded atrial and ventricular electrograms were subsequently digitized on a personal computer with an analog-to-digital system (Scientific Solutions, Inc.) at a sampling rate of 1000 Hz. The programs for digitization and subsequent waveform analysis were written in C programming language and Assembly language.

TABLE I
Patient Data

Pt	Age/Sex	Heart Disease	Drugs	SR/AF QRS Morphology	VT QRS Morphology
1	75/M	CAD	None	SR-Normal	RBB-*S/R*
2	78/M	CAD	None	SR-Normal	LBB-*S/L*
3a	63/M	CAD	None	SR-LBBB	LBB-*S/R*
3b					LBB-*S/L*
4a	52/M	CAD	None	AF-LBBB	LBB-*S/L*
4b					LBB-*S/L*
5a	82/M	CAD	Proc	SR-Normal	RBB-*I/R*
5b					LBB-*I/R*
6a	78/M	CAD	Proc	SR-Normal	RBB-*I/L*
7a	75/F	CAD	Am	SR-Normal	RBB-*S/L*
7b					RBB-*S/L*
8	72/F	None	Am	SR-Normal	RBB-*S/R*
9	65/M	CAD	Qu Me	SR-Normal	LBB-*S/L*
10a	62/M	CAD	Am	SR-LBBB	LBB-*S/L*
11	56/M	VHD	Am	SR-LBBB	LBB-*S/R*
12	73/M	CAD	Am Me	SR-LBBB	LBB-*I/R*
13	67/M	CAD	En	SR-LBBB	LBB-*I/L*
14	60/M	CAD	Qu Me	SR-RBBB	RBB-*S/R*
15	61/M	CAD	Proc	SR-RBBB	LBB-*S/R*
16a	84/M	CAD	Am	SR-IVCD	RBB-*I/R*
16b					RBB-*S/L*
17	74/M	CAD	Am	SR-IVCD	LBB-*S/L*
18a	68/M	CAD	Am	SR-IVCD	†RBB-*S/R*
18b					†LBB-*S/L*
18c					†LBB-*S/L*
18d					†RBB-*S/R*
18e					†RBB-*S/R*
10b*	62/M	CAD	Am En	SR-IVCD	RBB-*S/R*
10c					LBB-*I/L*
6b*	78/M	CAD	En Proc	AF-IVCD	RBB-*S/R*
19	61/M	CAD	Qu Di	AF-IVCD	RBB-*S/L*

CAD = Coronary Artery Disease, VHD = Valvular Heart Disease; Am = Amiodarone, Di = Digoxin, En = Encainide, Me = Mexiletene, Proc = Procainamide, Qu = Quinidine; SR = sinus rhythm, AF = atrial fibrillation; LBBB = left bundle branch block, RBBB = right bundle branch block, IVCD = nonspecific intraventricular conduction delay; LBB = left bunde branch morphology, RBB = right bundle branch morphology; *I* = inferior axis, IND = indeterminant, S = superior axis; *L* = leftward, *R* = rightward.

*These patients were studied on two different days with two different VT morphologies.

†This patient had five distinct VT morphologies.

Methods of Analysis

Data sets typically consisted of three 15 second passages from each patient. Two separate passages were digitized of ventricular signals during passages of the patient's underlying rhythm (sinus rhythm or atrial fibrillation). A third passage was digitized from a segment of induced monomorphic ventricular tachycardia. In some patients pacing intervention was required during VT be-

fore the full 15 s elapsed and shorter passages were used for analysis. The minimum number of depolarizations used for any VT passage was 20. Only 7 passages had fewer than 30 depolarizations. Any fusion depolarizations occurring during ventricular tachycardia were also included in the processing.

Each patient's initial sinus rhythm/atrial filtration passage was used to construct a ventricular waveform template for subsequent comparison to *each* normal depolarization during the second sinus rhythm/atrial fibrillation passage and *each* depolarization during a later passage of monomorphic ventricular tachycardia. The patient specific template was constructed by averaging all normal ventricular depolarizations in the initial sinus rhythm/atrial fibrillation passage and the size of the template was chosen to include only depolarization, as described previously [23]. The four detection algorithms were then evaluated for separation of the ranges for the similarity index ρ during the two rhythms of interest, normal ventricular conduction and conduction during ventricular tachycardia. Correlation waveform analysis was used as a reference for evaluating the similarity of each method.

Triggering: A software trigger was used for detection of waveforms. Two distinct methods were used for alignment of templates with waveforms in similarity analysis of these algorithms. Templates were initially aligned using peak amplitude and the appropriate similarity measure computed. Subsequently a *best fit* algorithm was used to maximally align the templates with the waveforms under analysis within an 11 ms window as described previously [23]. The location of the best alignment for one algorithm did not necessarily coincide with the best alignment for another algorithm.

Methods for Detection of Ventricular Tachycardia

In presenting the five algorithms which were evaluated for VT recognition, the following notation will be used:

N = the number of points in the template.
t_i = the template points.
s_i = the signal points to be processed.
$\bar{t}$ = the template average.
$\bar{s}$ = the signal average.
$\dot{t}_i$ = the first derivative of the template points.
$\dot{s}_i$ = the first derivative of the signal points.
ρ = the value of the similarity measure.

In each case in which the derivative was computed, the signal was first passed through a software low-pass filter (Hamming window, 21 points, cutoff 250 Hz) to remove extraneous noise. The derivative was then computed using a software differentiating filter (9 point Parks-McClellan differentiator, cutoff at 300 Hz). The differentiating filter had a cutoff beyond that of the cutoff of the low-pass filter to ensure that the derivative was correctly computed at all frequencies, even in those frequencies in the leakage areas of the low-pass filter. Both the differentiating and low-pass filtering operations are assumed to be performed in analog hardware in an eventual implementation of any of these techniques. Thus, computations required to perform these processes in software are not included in the analysis of computational cost for each method.

Correlation Waveform Analysis (CWA): Correlation waveform analysis employs the correlation coefficient ρ as a measure of similarity between the template and waveform under analysis [13], [23]. The correlation coefficient is independent of both amplitude fluctuations and baseline changes, and produces an output between -1 and 1. Mathematically, the correlation coefficient is defined as

$$\rho = \frac{\sum_{i=1}^{i=N} (t_i - \bar{t})(s_i - \bar{s})}{\sqrt{\sum_{k=1}^{k=N} (t_k - \bar{t})^2} \sqrt{\sum_{k=1}^{k=N} (s_k - \bar{s})^2}}. \quad (1)$$

To avoid computing the square root, we use the similarity measure

$$\rho = \text{sign}(\rho)\rho^2. \quad (2)$$

The correlation coefficient has been shown to produce a reliable metric for recognition of waveform changes. Thus, this well-established method is used as *standard* for evaluation of other techniques, as well as a basis for comparison of computational costs.

Bin Area Method (BAM): BAM compares corresponding area segments or *bins* constructed from the template with bins constructed from subsequent depolarizations using a simple norm. Consecutive sample points are summed to estimate the areas using a rectangular area rule in equal-sized bins. The average of these bin values is then removed resulting in a correction of baseline deviation, and these corrected bin values are normalized by the absolute sum of all corrected bin values. As a final step, the sum of the absolute difference of these normalized and corrected bins with an identically processed template is computed.

More simply, for 3-point bins, $S_1 = s_1 + s_2 + s_3$, $S_2 = s_4 + s_5 + s_6$, $\cdots$, $S_M = s_{N-2} + s_{N-1} + s_N$. For M bins the similarity measure is

$$\rho = 1 - \sum_{i=1}^{i=M} \left| \frac{T_i - \bar{T}}{\sum_{k=1}^{k=M} |T_k - \bar{T}|} - \frac{S_i - \bar{S}}{\sum_{k=1}^{k=M} |S_k - \bar{S}|} \right| \quad (3)$$

where $\bar{S} = (1/M) \sum_{k=1}^{k=M} S_k$.

BAM, like CWA, is independent of both baseline changes and amplitude fluctuations, and produces a similarity measure between -1 and 1 (1 being an ideal fit to the template).

Normalized Area of Difference (NAD): This method is identical to BAM except that the average bin value is not removed. By not removing the average value the algorithm avoids one division which would otherwise increase the computational demand each time the BAM algorithm is applied. NAD is independent of amplitude changes.

Derivative Area Method (DAM): DAM differs from CWA, BAM, and NAD by utilizing the first derivative of the electrogram waveform rather than the waveform itself. The zero crossings of the derivative of the template are used to partition the template and the same partitioning is applied to each subsequent waveform under analysis. The area beneath the derivative in each partition of the analyzed waveform is computed and compared to the corresponding area of the template. It is important to note that *the locations of the zero crossings of the derivative of the template are used to partition all subsequent waveforms under analysis.*

In order to force the segmenting of the derivative template on each subsequent depolarization, the following conceptual scheme is used (see Fig. 1). Starting at the beginning of the template, if the sign of the current derivative is the same as the sign of the previous derivative the value of "0" is stored in the zero crossing array (ZCA); whereas if the sign has changed, a "1" is stored. Template values $\dot{T}_k$ are computed by summing values of the derivative of the template $\dot{t}_i$ for each point which has a "0" in the ZCA array. When a "1" occurs in the ZCA, the current derivative value is included in the area, but a new summation begins for the subsequent area.

To process subsequent depolarizations, the ZCA constructed from the template is aligned with the depolarization and the area under the derivative, $\dot{S}_k$, is computed for the segments defined by the ZCA. In such a manner, the initial template partitioning is imposed on each depolarization under analysis. (See Fig. 2.)

As a final step, the similarity measure is given as follows:

$$\rho = 1 - \sum_{k=1}^{k=M} \left| \frac{\dot{T}_k}{\sum_{j=1}^{j=M} |\dot{T}_j|} - \frac{\dot{S}_k}{\sum_{j=1}^{j=M} |\dot{S}_i|} \right| . \qquad (4)$$

DAM produces a similarity measure between -1 and 1 (1 reflecting a good fit) and is independent of baseline changes and amplitude fluctuations.

Accumulated Difference of Slopes (ADIOS): ADIOS is similar to DAM in that it also employs the first derivative of the waveforms. This method was designed to exploit differences reflected by *notching* which may appear in the ventricular electrogram using sinus rhythm or ventricular tachycardia. A template is constructed of the *sign* of the derivative of the ventricular depolarization template. This template of *signs* is then compared to the *signs* of the derivative for subsequent depolarizations. The total number of sign differences between the template and the current ventricular depolarization is then computed as

$$\rho = \sum_{i=1}^{i=N} \text{sign}(\dot{t}_i) \oplus \text{sign}(\dot{s}_i) \qquad (5)$$

where $\oplus$ is the Exclusive-OR operator. The number of sign changes is bounded by 0 and the maximum number of points in the template (N), i.e., $\rho \in \{0, \cdots, N\}$. Since this method is based on the sign of the first derivative only, it is independent of baseline changes and amplitude differences between signals. It is the least computationally demanding algorithm of the five under consideration, requiring no multiplications nor divisions. In comparing the results for ADIOS to the other methods, the similarity measure ρ is mapped into the range $[-1, 1]$ using the mapping

$$\rho_{\text{mapped}} = 1 - \frac{2\rho}{N}. \qquad (6)$$

For each instance of ventricular tachycardia, the difference in the mean value of ρ for all ventricular tachycardia depolarizations was subtracted from the mean value of ρ for all normal depolarizations during the same patient's sinus rhythm passage. The average separation of the means is computed as

$$\overline{\delta\mu} = \frac{1}{31} \sum_{i=1}^{i=31} (\mu_i^{sr/af} - \mu_i^{vt}) \qquad (7)$$

where

$\overline{\delta\mu}$ = the average separation of the means.

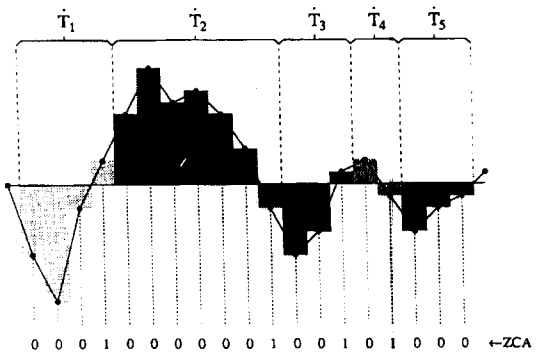

Fig. 1. Derivative of a waveform for construction of the template derivative areas $\dot{T}_k$ and the zero crossing array (ZCA) for use in the derivative area method (DAM).

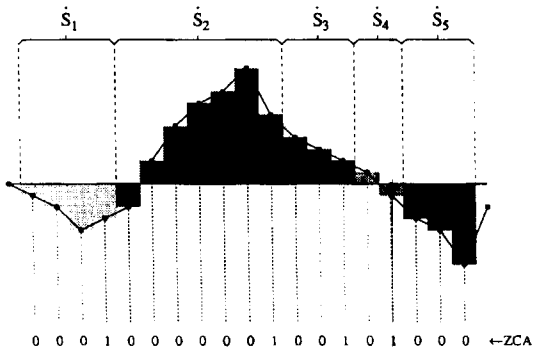

Fig. 2. Derivative of a waveform which is partitioned by the zero crossing array (ZCA) for construction of the signal derivative area $\dot{S}_k$ for use in the derivative area method (DAM).

$\mu_i^{sr/af}$ = the mean value of ρ for the ith passage of SR/AF.

μ_i^{vt} = the mean value of ρ for the ith passage of VT.

Finally, in processing the data with each of these methods, the initial templates were *identical* for CWA, DAM, ADIOS, and both BAM and NAD with 1 point bins. For DAM and ADIOS the first derivative of the common template was used. For BAM and NAD with 3 and 5 point bins, the window was extended as necessary to the left (towards onset of depolarization) to make all bins sizes in the template identical. For all algorithms under study, the initial alignment (triggering point) during sinus rhythm/atrial fibrillation and VT was identical. Thus, all algorithms compared used the same template (or the derivative of the template) and the same alignment point.

Results

The results of applying each of these methods to each of the VT passages and the corresponding SR/AF passage are summarized in Tables II and III for the original and best fit template alignment, respectively. If there was any overlap in the range of similarity index ρ computed for each depolarization during the VT passage with the range of similarity values computed for the corresponding SR/AF passage a "*" is entered in the tables. If there was no overlap in the ranges, the corresponding entry was blank. As Table II and III indicate, if one method failed for a patient, generally all methods failed for that patient.

The computational complexity of each method is summarized in Table IV. In addition, this table summarizes the total number of instances VT could be distinguished from SR/AF at both the original and best fit trigger location. The computational complexity reported is that required to apply each algorithm ones, i.e., to evaluate the match between the template and the waveform under analysis at one location. The results of averaging the *separation of the means* over the 31 VT passages are shown in Table IV. The average separation of the means is comparable for NAD, BAM, and DAM, and is larger than for CWA or ADIOS.

Fig. 3 presents the *average value* of each similarity measure during sinus rhythm and VT for CWA, BAM, NAD, and DAM for the best fit trigger points. In these figures, there are results from 31 VT passages and 21 SR/AF passages. In addition, there are a few instances where the VT or SR/AF means occurred at the same value so it is not possible to observe all of the mean values. Table V shows each method and the number of VT's which had mean values of the similarity measure ρ during any passage overlapping any of the mean values of the similarity measure during the sinus rhythm/atrial fibrillation passages for both the original and best fit alignment, respectively.

Correlation Waveform Analysis: CWA discriminated 27/31 (87%) and 28/31 (90%) VT's from sinus rhythm using the original and best fit trigger locations, respectively. The absolute maximum temporal distance from the original trigger to the best fit alignment between template and all subsequent sinus rhythm or atrial fibrillation depolarizations was 1 ms for 19/21 (91%) and 2 ms for the remaining two cases. Data processed with CWA generally had the highest mean value and smallest variance during sinus rhythm, but also has the second smallest *average separation* between sinus rhythm or atrial fibrillation and VT. As shown in Fig. 3, the mean values for CWA in sinus rhythm were generally much closer to 1 than for any other method. In a separate analysis with the template size fixed at 64 ms, CWA discriminated VT from sinus rhythm in 28/31 (90%) cases at the original trigger point. In this analysis, we used the correlation coefficient ρ directly, rather than ρ.

Bin Area Method: Depending on the number of points per bin, BAM discriminated 25/31 (81%) to 28/31 (90%) VT's from sinus rhythm or atrial fibrillation using the original and best fit trigger points. Of the three different bin sizes, a 1-point bin was slightly more effective in separating sinus rhythm or atrial fibrillation from ventricular tachycardia using the original trigger. Using a best fit alignment, 1- and 3-point bins were equally effective.

TABLE II
Results for Original Trigger Location

		BAM			NAD			
Pt	CWA	1pt	3pt	5pt	1pt	3pt	5pt	DAM
1	*	*	*	*				
2								
3a	*	*	*	*			*	*
3b			*	*			*	*
4a								
4b								
5a								
5b								
6a								
7a	*	*	*	*				*
7b								
8								
9		*	*	*				
10a								
11								
12								
13								
14								
15								
16a								
16b								
17								
18a								
18b								
18c								
18d								
18e								
10b								
10c								
6b	*	*	*	*				*
19								
Total Successes	27	26	25	25	31	31	29	27

A blank entry indicates no overlap in ranges of ρ indicating complete success in separation of every depolarization in VT from those in SR/AF. The "*" indicates some overlap. The total number of VT's with no overlap is shown in the last line of the table for each of the methods. Total success reflect the number of distinguished episodes out of the 31 possible.

TABLE III
RESULTS FOR BEST FIT TEMPLATE ALIGNMENT

		BAM			NAD				
Pt	CWA	1pt	3pt	5pt	1pt	3pt	5pt	DAM	ADIOS
1									*
2									*
3a	*	*	*	*				*	*
3b				*				*	*
4a									
4b									
5a									*
5b									*
6a									
7a	*	*	*	*			*		
7b				*	*	*	*		*
8									
9									*
10a									
11									
12									*
13									
14									
15									*
16a									
16b									
17									*
18a									
18b									
18c									
18d									*
18e									
10b									
10c									
6b	*	*	*	*				*	*
19									
Total Successes	28	28	28	26	30	30	29	28	18

A blank entry indicates no overlap in ranges of ρ indicating complete success in separation of every depolarization in VT from those in SR/AF. The "*" indicates some overlap. The total number of VT's with no overlap is shown in the last line of the table for each of the methods. Total successes reflect the number of distinguished episodes out of the 31 possible.

TABLE IV
COMPUTATIONAL COMPLEXITY AND RESULTS FOR 31 DIFFERENT VENTRICULAR TACHYCARDIAS

			Original Trigger		Best Fit Trigger	
Method	Multiplications	Divisions	SR/AF-VT Separation	$\overline{\delta\mu}$	SR/AF-VT Separation	$\overline{\delta\mu}$
CWA	$2N + 2$	1	27	0.575	28	0.444
BAM (1pt/bin)	$N + 1$	1	26	0.721	28	0.633
BAM (3pt/bin)	$N/3 + 1$	1	25	0.720	28	0.625
BAM (5pt/bin)	$N/5 + 1$	1	25	0.705	26	0.613
NAD (1pt/bin)	$N + 1$	0	31	0.735	30	0.653
NAD (3pt/bin)	$N/3 + 1$	0	31	0.742	30	0.654
NAD (5pt/bin)	$N/5 + 1$	0	29	0.732	29	0.648
DAM	M[†]	0	27	0.664	28	0.585
ADIOS	0	0	—	—	18	0.417

Separation indicates no overlap in the range of similarity values (ρ) during an instance of ventricular tachycardia compared to the ranges of similarity values during the corresponding sinus rhythm/atrial fibrillation (SR/AF) passages. $\overline{\delta\mu}$ is the average separation of the SR/AR and VT mean values for the 31 VT instances. The bound on ρ for ADIOS was scaled to a range of -1 to 1. N = the number of points in the template, M = the number of partitions of the waveform. All methods assume a threshold γ has been determined and all template processing has been performed in advance.

[†]For the patients studied, $M \leq N/4$.

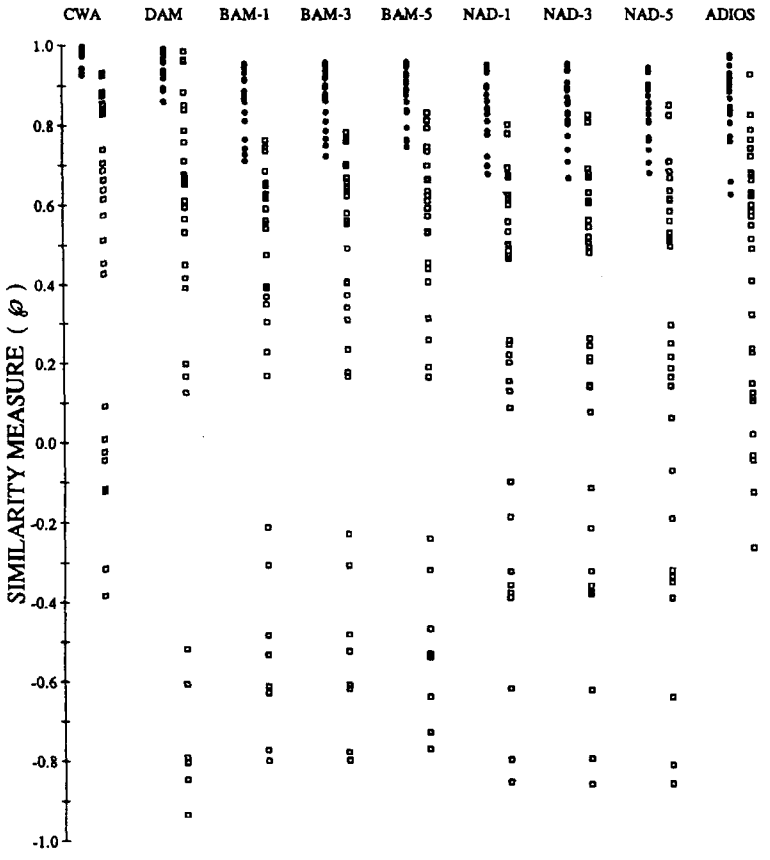

Fig. 3. Average values of the similarity measure (ρ) for each passge of sinus rhythm/atrial fibrillation (●) and ventricular tachycardia (□) for CWA, BAM with 1-, 3-, and 5-point bins, NAD with 1-, 3-, and 5-point bins, and DAM using the best fit alignment.

For 1-, 3-, and 5-point bins, the maximum absolute temporal distance from the original trigger to the best fit alignment between template and subsequent sinus rhythm or atrial fibrillation depolarizations was 1 ms for 18/21 (86%), 19/21 (91%), and 17/21 (81%) cases, respectively. This value was 2 ms for the remaining cases. Even three computations of BAM (one at the original trigger point and at one point to either side) with 3- or 5-point bins requires considerably less time than computing the correlation coefficient at the original trigger point. Data processed with BAM generally had a larger variation in sinus rhythm range than CWA and DAM, but was much less computationally demanding than CWA.

Normalized Area of Difference: NAD discriminated 31/31 (100%) to 29/31 (94%) VT's from sinus rhythm or atrial fibrillation using the original and best fit trigger locations. For 1-, 3-, and 5-point bins, the maximum absolute temporal distance from the original trigger to the best fit alignment between template and subsequent sinus rhythm or atrial depolarizations was 1 ms for 18/21 (86%), 16/21 (76%), and 15/21 (71%) cases, respectively. This value was 2 ms for the remaining cases. Since this algorithm requires no real-time divisions, computing ρ at the original trigger point and at 1 or 2 points to either side of the original trigger point requires fewer computations than computing the correlation coefficient at the original trigger location. Data processed using NAD generally showed a larger variation in sinus rhythm values than CWA, DAM, and BAM. However, this method was the most effective of the five in discriminating sinus rhythm from ventricular tachycardia overall, and also had the largest average separation of the means.

Derivative Area Method: DAM discriminated 27/31 (87%) and 28/31 (90%) VT's from sinus rhythm or atrial fibrillation using the original and best fit trigger locations, respectively. The maximum absolute temporal distance from the original trigger to the best fit alignment between template and subsequent sinus rhythm or atrial fibrillation depolarizations was 1 ms in 8/21 (38%) cases, 2 ms in 6/21 (27%) cases, and 3–5 ms in the remaining 7 cases.

TABLE V
NUMBER OF VENTRICULAR TACHYCARDIA EPISODES (OUT OF 31 POSSIBLE) WITH MEAN VALUES OF THE SIMILARITY MEASURE (ρ) FOR A PASSAGE EXCEEDING THE MEAN VALUE OF THE SIMILARITY MEASURE FOR ANY OF THE SINUS RHYTHM PASSAGES

Method	Original Trigger	Best Fit Alignment
CWA	0	2
BAM (1pt/bin)	1	3
BAM (3pt/bin)	2	3
BAM (5pt/bin)	2	4
NAD (1pt/bin)	2	2
NAD (3pt/bin)	2	5
NAD (5pt/bin)	1	3
DAM	6	4
ADIOS	–	11

Results using DAM were similar to those of CWA. While DAM does not have a predefined number of multiplications, for the patients studied the number of multiplications was always less than 1/8 that required by CWA. DAM had the second smallest range of mean values during sinus rhythm but also had good average separation of the sinus rhythm and ventricular tachycardia mean values.

Accumulated Difference of Slopes: ADIOS discriminated 18/31 (58%) VT's from sinus rhythm or atrial fibrillation using the best fit trigger. Because this method is sensitive to correct alignment between the template and the waveform under analysis, the original trigger was not used. ADIOS was the least computationally demanding method, but also the least effective (on average). However, since this algorithm did not require multiplications nor divisions the computational cost of sliding the template to achieve a best fit is undemanding. The results of this algorithm, using an overlap/no overlap performance criteria, were unimpressive.

DISCUSSION

Since activation as seen by a closely spaced bipolar pair is sensitive primarily to the *direction* of activation traversing the axis of the pair, the premise of this study is that abnormal depolarization will display a different morphology by virtue of its different conduction pathway. This is not always the case when recording from an electrode which exhibits such a proximity effect.

Results showed that no single discriminant boundary derived from any of the four methods can separate all ventricular depolarizations during sinus rhythm (or atrial fibrillation) from those during ventricular tachycardia. Patient specific thresholds were necessary to ensure optimal separation. In actual implementation, not all VT must be separated from all SR/AF depolarizations, and looser thresholds might be allowed. Based on the results of this study, it might be possible to determine the range of similarity values ρ during a 15 s passage of SR/AF and set the detection threshold at the minimum ρ obtained during the SR/AF passage.

In addition, injury current produced by acutely placed electrode catheters can affect results when using fixed sized windows as reported previously [13], [19]–[22]. While fixed sized templates may be preferable once permanent leads are implanted, we purposely used patient-specific template sizes to avoid inclusion of acute injury current in this study. Further work needs to be done to determine whether the inclusion of repolarization might result in greater discriminatory ability once acute injury current subsides. However, this can only be determined from chronic leads. Unfortunately, there are currently no methods available for examining digital waveforms from chronic devices, particularly at the resolution required for this analysis.

Applying a fixed 64 ms template such as proposed by Lin *et al.* [13] to our series of patients, CWA (using the true correlation coefficient ρ, rather than ρ) separated sinus rhythm from VT in 28/31 (90%) cases using our proposed patient-specific thresholds. However, VT correlation coefficient values in 14/31 (45%) instances *exceeded* 0.90, above the single discriminant boundary found to be successful in the earlier Lin study. Differences may be due to the distinct patient populations of the two studies (there was no overlap between the patients used by Lin and those used in this study). In contrast to the observations in Lin's earlier study, the present study suggests that a universal threshold for separating VT from SR cannot be expected using CWA.

An important feature of BAM is the simplicity of computation (on average $\frac{1}{6}$ that of CWA). The realignment of the waveform with the template showed that a best fit occurred within ± 1 ms of the original trigger point for 91% of all depolarizations in the 3-point bin case. Thus, three calculations of BAM could be expected to yield excellent results and still give a computational reduction of $\frac{1}{2}$ when compared to a single calculation of CWA.

DAM and ADIOS are based on the first derivative of the ventricular waveform, as is the gradient pattern detection (GPD) algorithm of Davies *et al.* [14]–[16]. The GPD algorithm discriminates waveforms based on the order in which the first derivative crosses predetermined thresholds. Such crossings are directly dependent on the amplitude of the waveforms; hence, modest fluctuations in amplitude may cause ventricular depolarizations with identical morphology to be classified differently. Our technique differs from theirs in that the ZCA derived from the template is imposed upon all subsequent waveforms. This serves to emphasize even subtle differences between the waveforms during sinus rhythm (or atrial fibrillation) and the waveform during VT, and results in better performance in the case of small but real differences in the waveform only, disregarding amplitude changes. More importantly, there is no well-defined discriminant measure in the GPD algorithm to determine how closely a waveform matches the template, i.e., there appears to be no general means for setting thresholds for detecting ventricular tachycardia using the GPD algorithm. In contrast, both DAM and ADIOS produce bounded error measures indicating the relative similarity of the template and the waveform under analysis. Such a bounded measure is cru-

cial to selection of robust discriminant boundaries for final implementation.

The poor results from ADIOS were due in part to the fact that this algorithm generates an integer corresponding to the number of sign differences between the template and the derivative of the current depolarization, (i.e., $\rho \in \{0, \cdots, N\}$). In two cases, the largest ρ in sinus rhythm (or atrial fibrillation) was identical to the lowest ρ in VT, so the method was declared to have failed. In fact, only 3/38 VT depolarizations in one patient and 1/40 VT depolarizations in the other patient were responsible for this coincidence of values. In three other cases, the VT range overlapped the highest sinus rhythm value by a single integer. Since both DAM and ADIOS utilize the first derivative of the ventricular waveform, we submit that the application of ADIOS as a first pass followed by DAM when VT is not positively identified may be a rapid and computationally effective sequential method for detecting VT. If ADIOS detects VT, there is no need for further analysis; while if ADIOS cannot reliably detect VT, DAM can be applied as a second pass for increased sensitivity. The combination of the two techniques matches the performance of CWA, but the combined computational cost of ADIOS/DAM is still less than $\frac{1}{8}$ that of CWA.

BAM and NAD are similar to the area of difference method used by another group of investigators [19]–[22]. The area of difference algorithm is computationally very simple, requiring no multiplications nor divisions. However, this simplistic method can be affected by baseline and amplitude fluctuations such that depolarizations identical in morphology may be misclassified [22]. In contrast, BAM and NAD are independent of amplitude fluctuations. In addition, we impose a normalization scheme which serves to bound the output ($-1 \leq \rho < 1$).

Our criteria for success versus failure in this study were particularly exacting. If even a single depolarization from one class (SR/AF or VT) fell within the range of the other class, the test was considered to have failed for that patient. In actual implementation this requirement could conceivably be relaxed with the use of statistical methods such that only a certain percentage of consecutive depolarizations would be required to meet the criterion for VT detection.

At the 1000 Hz sampling rate, 100% of all *best fit* alignments for CWA, BAM, and NAD fell within ± 2 ms of the original trigger (peak). There was generally a slight improvement in separation of VT from SR/AF using the best fit alignment, but this was usually due to improved alignment of only one or two depolarizations. Using DAM, the best fit alignment occurred within ± 2 ms in 65% of the cases. However, results using DAM at the original trigger were identical to those of CWA and superior to the results using BAM. The results at the best fit were identical for DAM, CWA, and BAM with 1- and 3-point bins.

Limitations

The present study examined only electrograms from the distal tip of bipolar electrodes with a 1 cm spacing during clinical cardiac electrophysiology studies. Electrograms recorded with a different electrode configuration or recorded from the epicardium may produce different results and improve (or degrade) the ability to detect VT. Second, the selection of patient specific thresholds presents a difficult problem in the actual implementation of these algorithms. Future work in this area is necessary to determine the number of SR/AF depolarizations that need to be observed in order to set a reliable threshold. We chose to examine 15 s passages in this study because most patients could tolerate VT for this length of time without hemodynamic collapse. This allowed a significant number of VT depolarizations to be tested to be fairly confident that these algorithms could distinguish a large number of VT depolarizations from sinus rhythm or atrial fibrillation. Third, we tested monomorphic VT and did not examine the results using polymorphous VT or ventricular fibrillation. However, these template-matching algorithms are designed to be used in conjunction with rate-based algorithms to increase antitachycardia device specificity. Since ventricular fibrillation will occur at a high ventricular rate, we assume a rate detection algorithm will override any morphology information these algorithms might provide. Finally, the present study did not examine the effects of antiarrhythmic drugs on the morphology of the ventricular depolarizations. To compensate for such potential changes in the chronic situation, new ventricular templates may occasionally need to be constructed.

SUMMARY

In order to achieve real-time cycle-to-cycle analysis of ventricular electrograms during both sinus rhythm and ventricular tachycardia, computationally efficient algorithms will be crucial. In this study, four new time-domain algorithms were developed and evaluated on clinical electrophysiology data. The best discrimination of VT from sinus rhythm or atrial fibrillation occurred using NAD. Three other algorithms, CWA, BAM, and DAM, were also effective, though slightly less so than NAD. ADIOS was the least impressive of the group but may be found to be a good first pass method with the companion DAM as a followup. The most computationally demanding method is CWA, which has been used for over two decades as a classic technique for analysis of surface ECG's. Because of this acceptance as a morphological discriminant, it was used as our reference for the new techniques as well as for a comparison of relative computational costs. BAM, DAM, and NAD exhibited discriminatory power equivalent to CWA with computational requirements in the range of an order of magnitude lower. In addition, the average separation of the sinus rhythm mean compared to the corresponding mean during ventricular tachycardia was considerably larger with these methods than for CWA. ADIOS was the most computationally efficient algorithm, but with results trailing dramatically behind the other methods. It had a very low false positive rate though, and should be considered as a first pass screening method with good true positive detection

of VT. These new amplitude independent techniques provide ventricular electrogram analysis with computational efficiency consistent with power limitations of modern antitachycardia devices, while maintaining the discriminatory capability of CWA, an established method of waveform discrimination.

REFERENCES

[1] J. D. Fisher, M. Goldstein, E. Ostrow, J. A. Matos, and S. G. Kim, "Maximal rate of tachycardia development: Sinus tachycardia with sudden exercise vs. spontaneous ventricular tachycardia," *PACE*, vol. 6, pp. 221-228, Mar.-Apr. 1983.

[2] A. Geibel, M. Zehender, and P. Brugada, "Changes in cycle length at the onset of sustained tachycardias—Importance for antitachycardia pacing," *Amer. Heart J.*, pp. 588-592, Mar. 1988.

[3] M. Fromer, T. Kus, M. Dubuc, R. Nadeau, and M. Shenasa, "Oscillation of ventricular tachycardia cycles length," (abstract), *PACE*, vol. 10, p. 451, Mar.-Apr. 1987.

[4] A. W. Nathan, J. E. Creamer, D. W. Davies, and J. E. Camm, "Clinical experience with a new versatile, software based, tachycardia reversion pacemaker," *J. Amer. Col. Cardiol.*, (abstract), vol. 7, no. 2, p. 184A, Feb. 1986.

[5] W. H. Olson and G. H. Bardy, "Cycle length and morphology at the onset of spontaneous ventricular tachycardia and fibrillation," (abstract), *PACE*, vol. 9, p. 284, Mar.-Apr. 1986.

[6] W. Olson, G. Bardy, R. Mehra, C. Almquist, and R. Biallas, "Comparison of different onset and stability algorithms for detection of spontaneous ventricular arrhythmias," (abstract), *PACE*, vol. 10, p. 439, Mar.-Apr. 1987.

[7] ——, "Onset and stability for ventricular tachycardia detection in an implantable pacer-cardioverter-defibrillator," *IEEE Comput. Cardiol.*, pp. 167-170, 1987.

[8] G. Tomaselli, M. Scheinman, and J. Griffin, "The utility of timing algorithms fo distinguishing ventricular from supraventricular tachycardias," (abstract), *PACE*, vol. 10, p. 415, Mar.-Apr. 1987.

[9] J. Warren and R. O. Martin, "Clinical evaluation of automatic tachycardia diagnosis by an implanted device," (abstract), in *Proc. Cardiostim 86*, vol. 4, 1986, p. 16.

[10] K. L. Ripley, T. E. Bump, and R. C. Arzbaecher, "Evaluation of techniques for recognition of ventricular arrhythmias by implanted devices," *IEEE Trans. Biomed. Eng.*, vol. 36, no. 6, pp. 618-624, June 1989.

[11] M. Mirowski, M. M. Mower, and P. R. Reid, "The automatic implantable defibrilator," *Amer. Heart J.*, vol. 100, no. 6, pp. 1089-1092, Dec. 1980.

[12] M. Mirowski, M. M. Mower, P. R. Reid, L. Watkins, and A. Langer, "The automatic implanatable defibrillator: New modality for treatment of life-threatening ventricular arrhythmias," *PACE*, vol. 5, pp. 384-401, May-June 1982.

[13] D. Lin, L. A. DiCarlo, and J. M. Jenkins, "Identification of ventricular tachycardia using intracavitary ventricular electrograms: Analysis of time and frequency domain patterns," *PACE*, vol. 11, part 1, pp. 1592-1606, Nov. 1988.

[14] D. W. Davies, R. J. Wainwright, M. Tooley, D. Loyd, and A. J. Camm, "Electrogram recognition by digital analysis: Relevance to pacemaker arrhythmia control," (abstract), *J. Amer. Coll. Cardiol.*, vol. 5, no. 2, p. 507, Feb. 1985.

[15] D. W. Davies, R. J. Wainwright, M. A. Tooley, D. Lloyd, A. W. Nathan, R. A. J. Spurrell, and A. J. Camm, "Detection of pathological tachycardia by analysis of electrogram morphology," *PACE*, vol. 9, pp. 200-208, Mar.-Apr. 1986.

[16] D. W. Davies, M. A. Tooley, T. Cochrane, A. W. Nathan, R. J. Wainwright, and A. J. Camm, "Real-time tachycardia diagnosis using morphological analysis of electrograms," (abstract), *PACE*, vol. 10, p. 998, July-Aug. 1987.

[17] D. Santel, R. Mehra, W. Olson, and G. Bardy, "Integrative algorithm for detection of ventricular tachyarrythmias from the intracardiac electrogram," *IEEE Comput. Cardiol.*, pp. 175-177, 1987.

[18] F. Pannizzo and S. Furman, "Pattern recognition for tachycardia detection: A comparison of methods," (abstract), *PACE*, vol. 10, p. 999, July-Aug. 1987.

[19] J. L. Langberg, W. J. Gibbs, D. M. Auslander, and J. C. Griffin, "Identification of ventricular tachycardia with use of the morphology of the endocardial electrogram," *Circulation*, vol. 77, no. 6, pp. 1363-1369, June 1988.

[20] G. F. Tomaselli, A. P. Nielsen, W. L. Finke, L. Sengupta, J. C. Clark, and J. C. Griffin, "Morphologic differences of the endocardial electrogram in beats of sinus and ventricular origin," *PACE*, vol. 11, pp. 254-262, Mar. 1988.

[21] J. C. Griffin, J. Langberg, G. Tomaselli, and W. Gibbs, "Endocardial electrogram morphology: A unique characteristic of cardiac rhythm?," (abstract), in *Cardiostim 86*, vol. 4, 1986, p. 15.

[22] G. Tomaselli, W. J. Gibbs, J. J. Langberg, M. C. Chin, and J. C. Griffin, "In vivo testing of a morphology based approach to cardiac rhythm identification," (abstract), *Circulation*, vol. 76, p. 1116, 1987.

[23] R. D. Throne, J. M. Jenkins, S. A. Winston, C. J. Finelli, and L. A. DiCarlo, "Discrimination of retrograde from anterograde atrial activation using intracardiac electrogram waveform analysis," *PACE*, vol. 12, pp. 1622-1630, 1989.

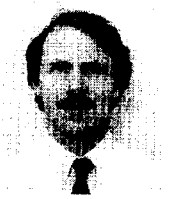

Robert D. Throne received the B.S. degree in mathematics and then electrical engineering from M.I.T., Cambridge, MA, in 1980 and 1985, and the M.S.E. and Ph.D. degrees in electrical engineering from the University of Michigan, Ann Arbor, in 1987 and 1990.

He is currently a Visiting Assistant Professor at the Pritzker Institute of Medical Engineering at the Illinois Institute of Technology, Chicago. His research interests are in signal processing of biological signals and control system theory.

Janice M. Jenkins (S'75-M'78-SM'84) received the B.S. degree in mathematics and computer science, and the M.S. and Ph.D. degrees in computer engineering from the University of Illinois at Chicago in 1974, 1976, and 1978, respectively.

She was a member of the faculty of Northwestern University, Evanston, IL, from 1979 to 1980, with an appointment in Internal Medicine and in Electrical Engineering and Computer Science. She is currently an Associate Professor of Electrical Engineering and Computer Science at the University of Michigan, Ann Arbor, a member of the Bioengineering faculty, and Director of the Medical Computing Laboratory, and the Digital Design Laboratory. Her research interests are digital signal processing of the electrocardiogram, and implantable devices for treatment of cardiac arrhythmias.

Lorenzo A. DiCarlo received the M.D. degree from the Tufts University School of Medicine, Boston, MA, and his training in Internal Medicine at the Hospital of the University of Pennsylvania in Philadelphia. His fellowships in Cardiology and Cardiac Electrophysiology were completed at the University of California, San Francisco.

He is the Director of the Cardiac Electrophysiology Laboratory at St. Joseph Mercy Hospital, Ann Arbor, MI. He also has joint appointments as an Adjunct Research Scientist in the Department of Electrical Engineering and Computer Science and as a member of the clinical faculty of the Department of Medicine at the University of Michigan. Active in clinical research, he has authored numerous articles in the diagnosis and treatment of heart rhythm disturbances, cardiac pacing, and device technology for the treatment of rapid heart rhythm disturbances.